Supplemental Data

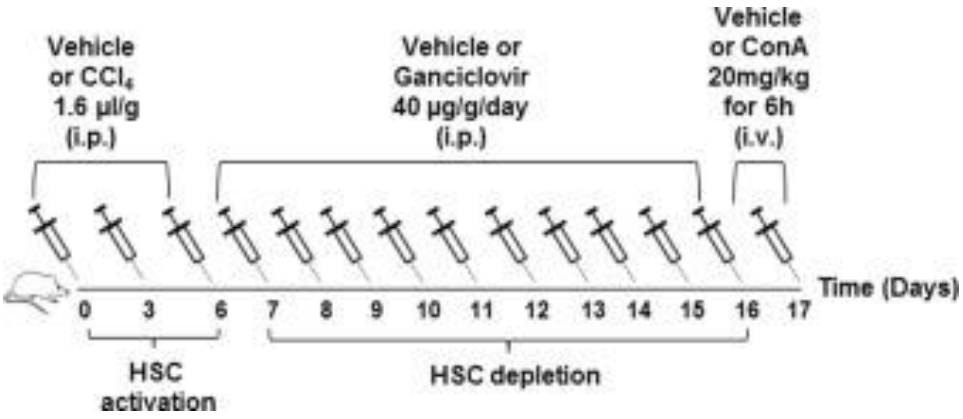

Supplemental Figure S1. Schematic presentation of the experimental design for *in vivo* hepatic stellate cell depletion and ConA treatment.

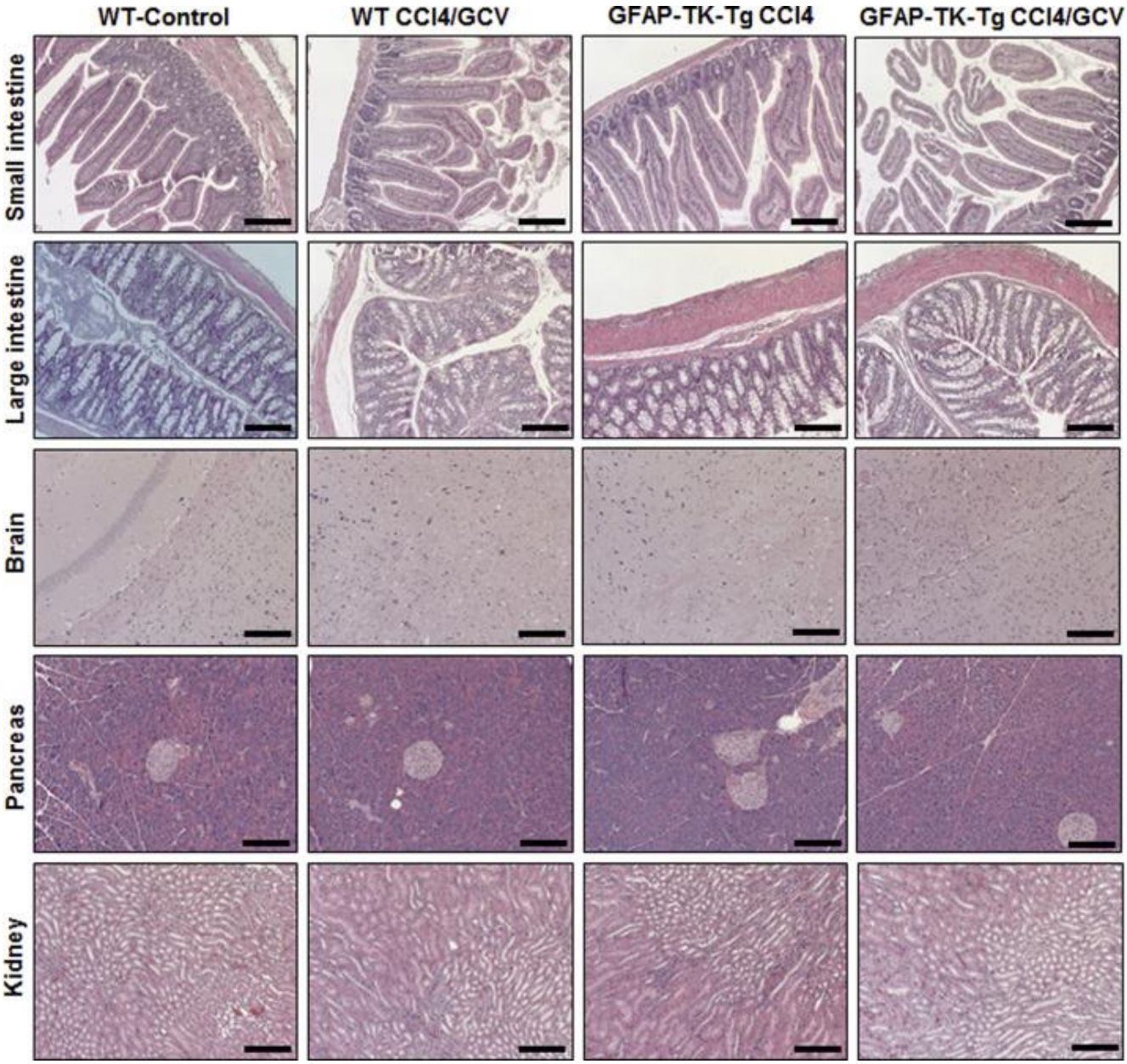

Supplemental Figure S2. WT or GFAP-TK-Tg mice were administered carbon tetrachloride (three administrations, 3 days apart). Carbon tetrachloride was then terminated, and treatment with ganciclovir (GCV) or PBS (control) was given for 10 days. Carbon tetrachloride treatment causes liver injury, which induces HSCs to enter the cell cycle. Incorporation of GCV metabolite (because of thymidine kinase) into replicating DNA causes death of HSCs. The liver injury due to earlier carbon tetrachloride treatment is abated, but HSCs are depleted from the GFAP-TK-Tg mice (which express thymidine kinase under the GFAP promoter) but not WT mice. The protocol did not cause any injury to the small intestine, large intestine, brain, pancreas, or kidney of WT or GFAP-TK-Tg mice. Scale bar = 100 μm.

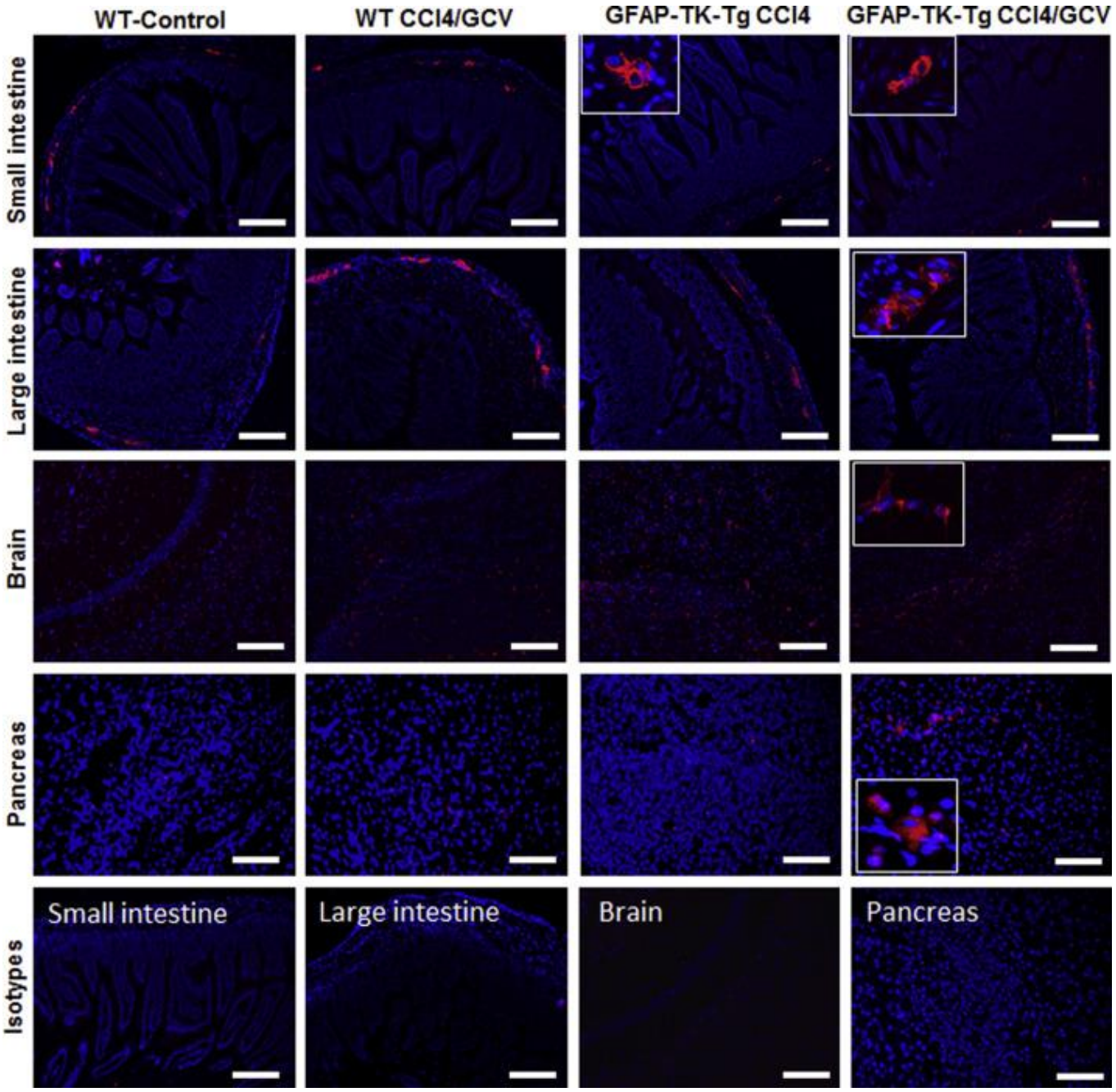

Supplemental Figure S3. Carbon tetrachloride, followed by ganciclovir (GCV), treatment of WT or GFAP-TK-Tg mice does not cause depletion of $GFAP^+$ cells in nonliver organs (small intestine, large intestine, brain, and pancreas). The **insets** demonstrate $GFAP^+$ cells at higher magnification. Scale bar = 100 μm. Original magnification: ×20 (**insets**).

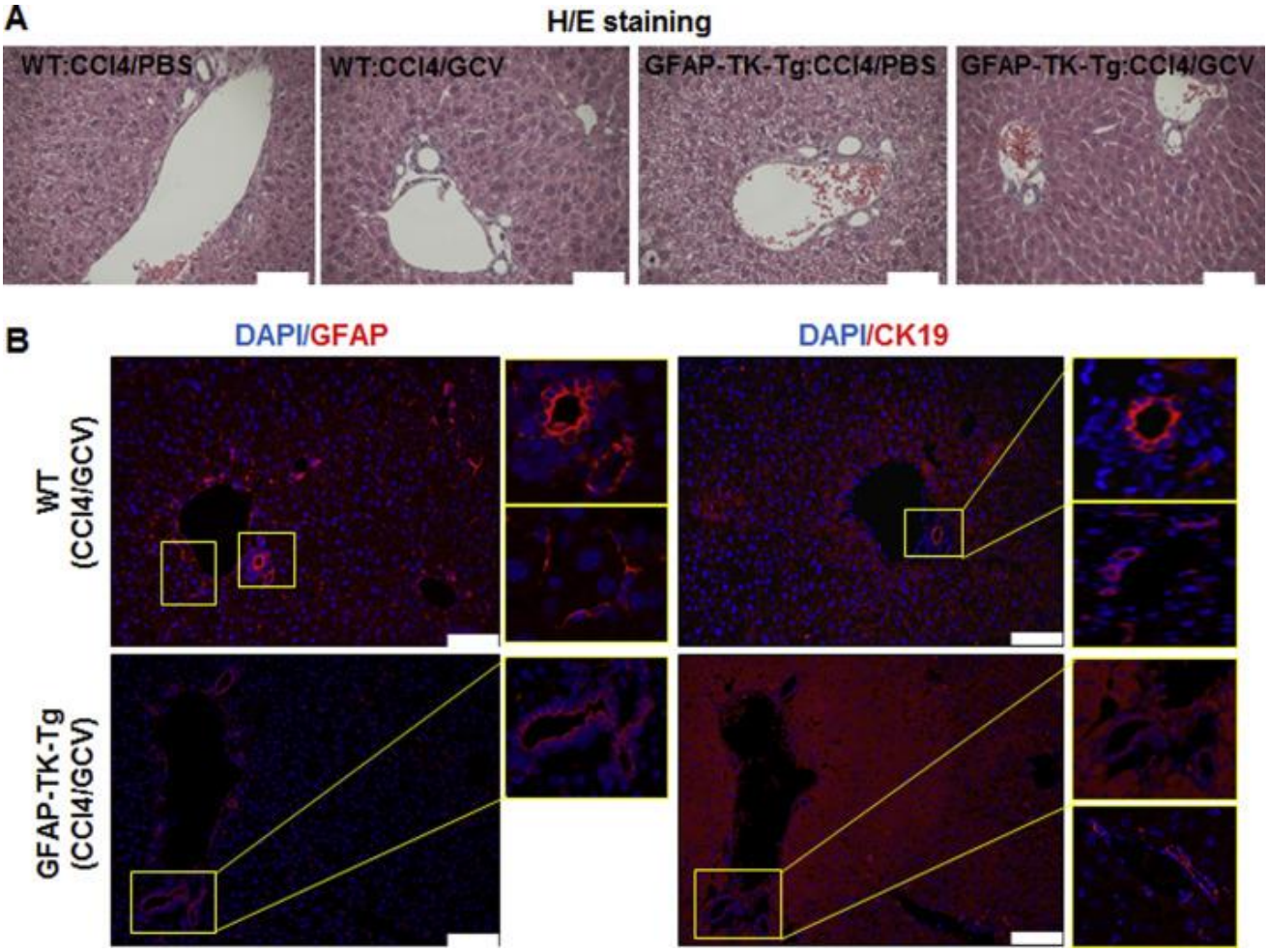

Supplemental Figure S4. WT or GFAP-TK-Tg mice were treated with carbon tetrachloride, followed by GCV. **A:** Carbon tetrachloride, followed by ganciclovir (GCV), treatment shows no hepatic injury, as determined by histopathological examination of hematoxylin and eosin (H&E)–stained liver sections of B6-WT or GFAP-TK-Tg mice. **B:** Depletion of $GFAP^+$ HSCs, but not $GFAP^+$ or $CK19^+$ cholangiocytes, is apparent in GFAP-TK-Tg mice treated with carbon tetrachloride, followed by GCV; B6-WT mice treated similarly retain $GFAP^+$ HSCs as well as $GFAP^+$ plus $CK19^+$ cholangiocytes. Images at high magnification of the marked **boxed areas** in **B** also show CK19 or GFAP staining more clearly. Scale bar = 50 μm (**A** and **B**). Original magnification: ×20 (**B**, **boxed areas**).

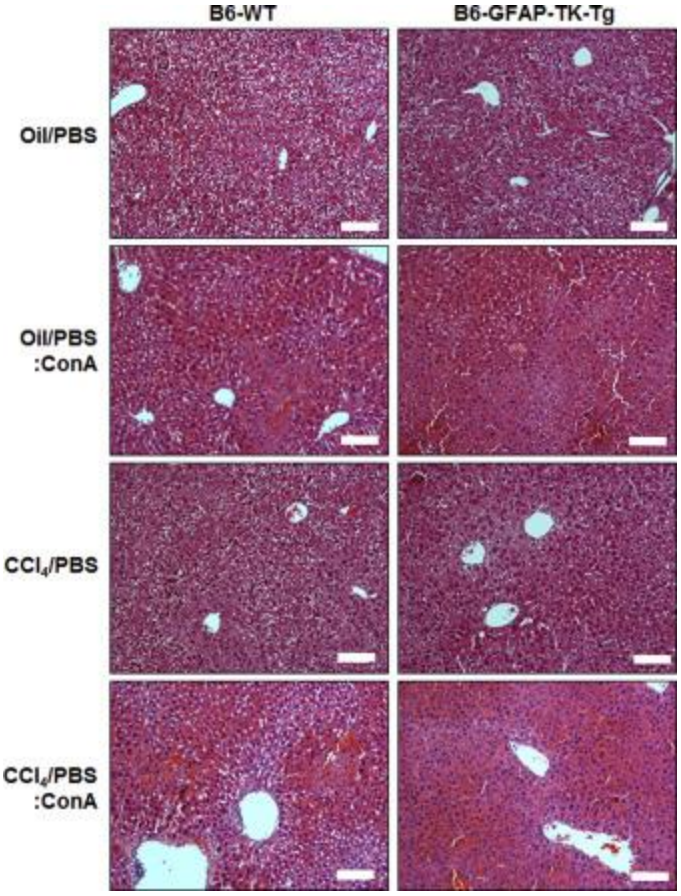

Supplemental Figure S5. WT or GFAP-TK-Tg mice were treated with carbon tetrachloride (three administrations, 3 days apart). This was followed by termination of carbon tetrachloride and treatment with PBS for 10 days. Mice were then injected ConA or vehicle (PBS) and euthanized 6 hours later. Vehicle (oil/PBS) or carbon tetrachloride treatment, followed by ConA treatment, shows similar hepatic injury, as determined by histopathological examination of hematoxylin and eosin–stained liver sections of B6-WT or GFAP-TK-Tg mice. Scale bar = 100 μm.

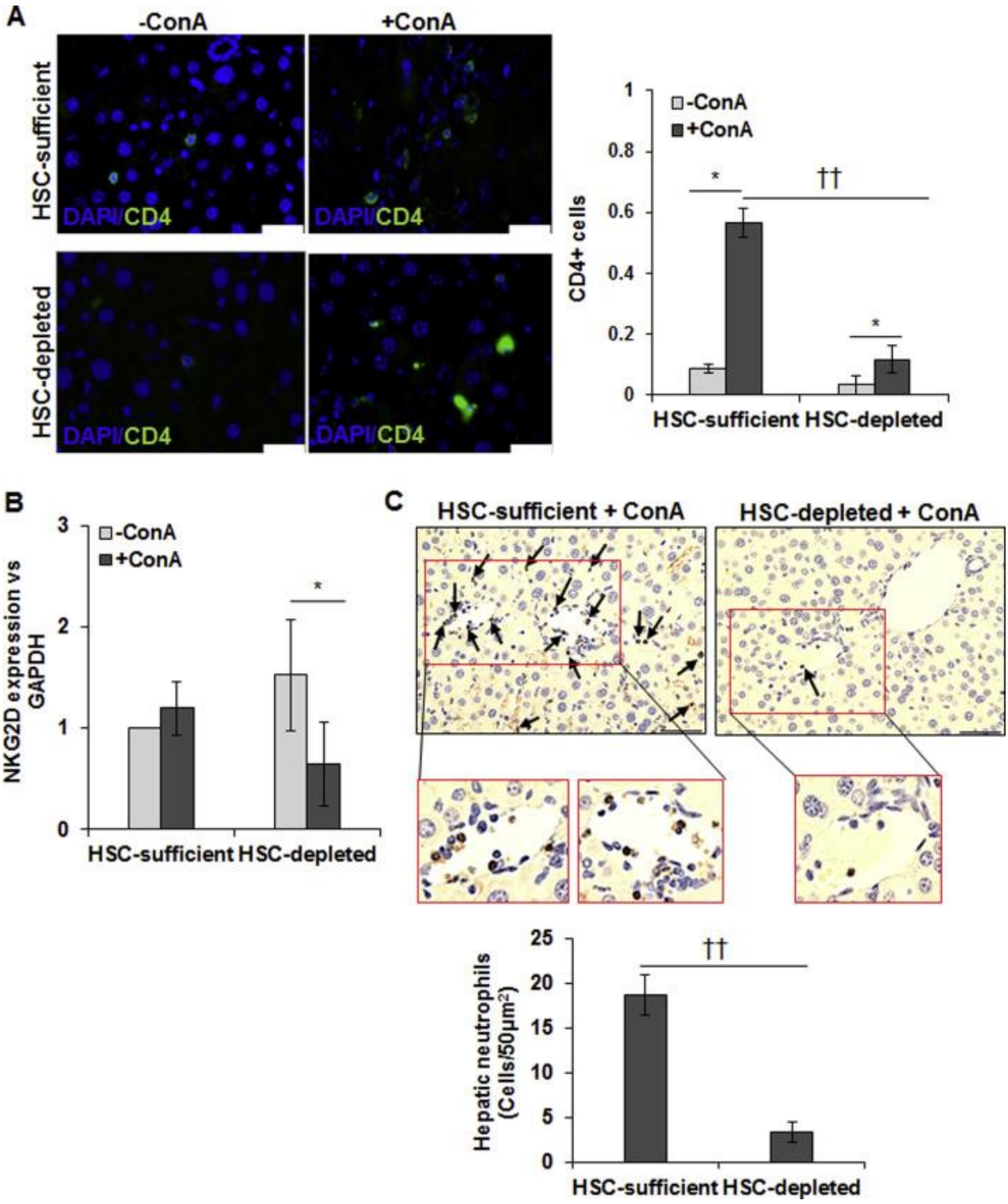

Supplemental Figure S6. CD4, NKT cells, and neutrophils in ConA-treated HSC-depleted mouse liver. **A:** Representative sections of the vehicle- or ConA-treated livers stained with anti-CD4 Ab. Few $CD4^+$ T cells are seen in vehicle-treated HSC-sufficient livers, and their number increases on ConA treatment. HSC-depleted mice do not show any $CD4^+$ T cells, and their

accumulation also is much lower after ConA. **B:** Quantitative real-time RT-PCR shows natural killer group 2D receptor (NKG2D) mRNA expression in ConA-treated HSC-sufficient and HSC-depleted mice. **C:** Robust hepatic neutrophil infiltration can be seen in the ConA-treated HSC-sufficient mice but not in HSC-depleted mice. Images at higher magnification of the **boxed areas** in **left** and **right panels** of **C** are also shown (**solid black arrows** indicate infiltration of neutrophil). Data are expressed as means ± SD. $n = 3$ mice per group (**C**). $^{*}P < 0.05$ versus control; $^{\dagger\dagger}P < 0.01$ versus HSC-depleted mice. Scale bar = 50 μm (**A** and **C**). Original magnification: ×20 (**C, boxed areas**). GAPDH, glyceraldehyde-3-phosphate dehydrogenase.

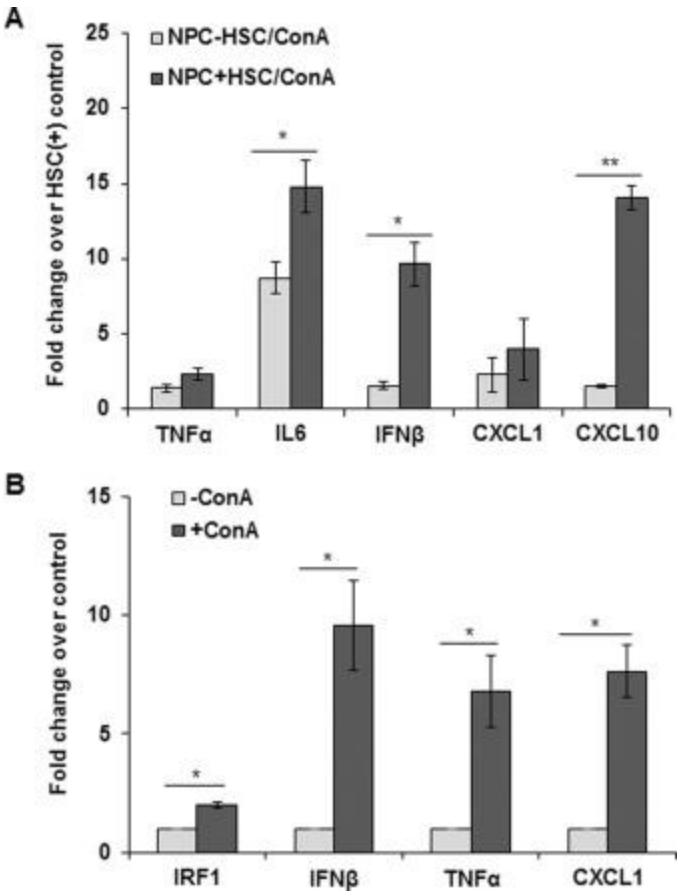

Supplemental Figure S7. **A:** Nonparenchymal cells (NPCs) were incubated without or with HSCs (10:1) for 8 hours in a medium containing 50 μg/mL ConA, and mRNA expression of tumor necrosis factor (TNF)-α, IL-6, interferon (IFN)-β, CXCL1, and CXCL10 was analyzed via quantitative real-time RT-PCR (RT-qPCR). **B:** HSCs were incubated for 8 hours in a medium containing 50 μg/mL ConA and were analyzed for IRF1, IFN-β, TNF-α, and CXCL1 mRNA expression via RT-qPCR. Data are expressed as means ± SD. $^{*}P < 0.05$, $^{**}P < 0.01$.

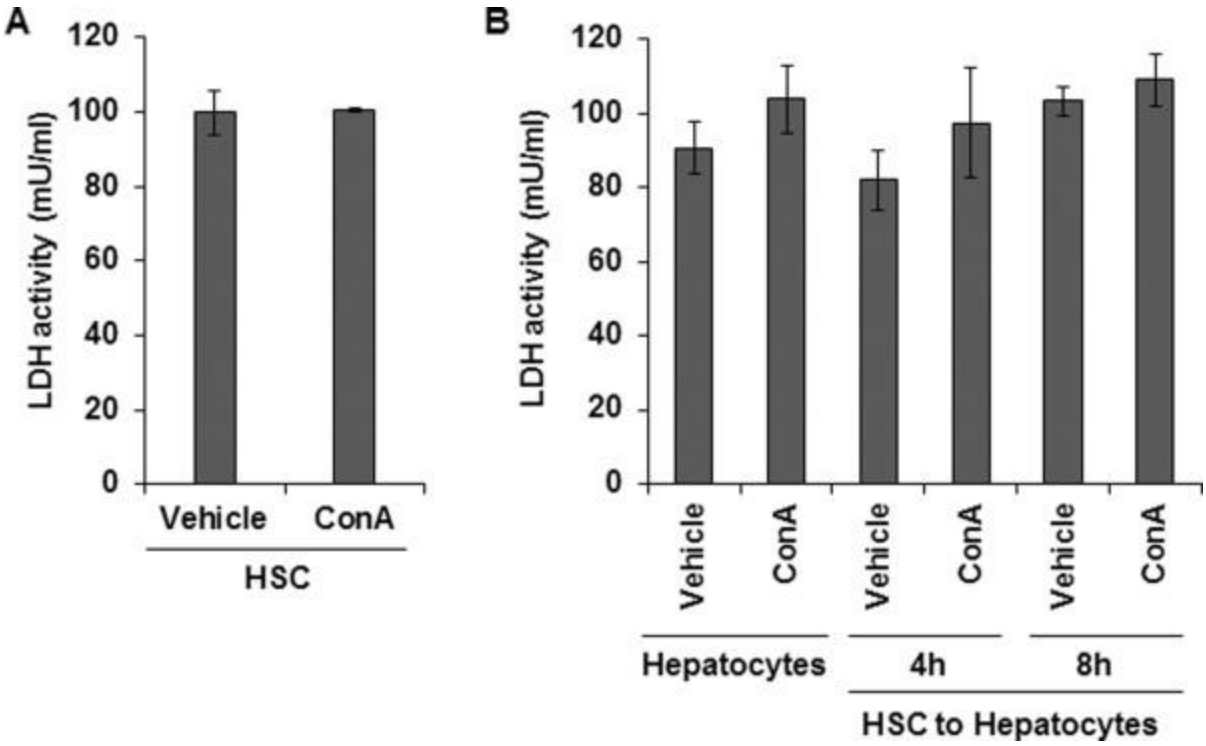

Supplemental Figure S8. Membrane damage was evaluated by lactate dehydrogenase (LDH) release from HSCs incubated in medium containing 50 μg/mL ConA for 6 hours (**A**) and hepatocytes incubated in medium containing ConA or medium conditioned by HSCs in the absence or presence of ConA for 4 and 8 hours (**B**). Data are expressed as means ± SD.

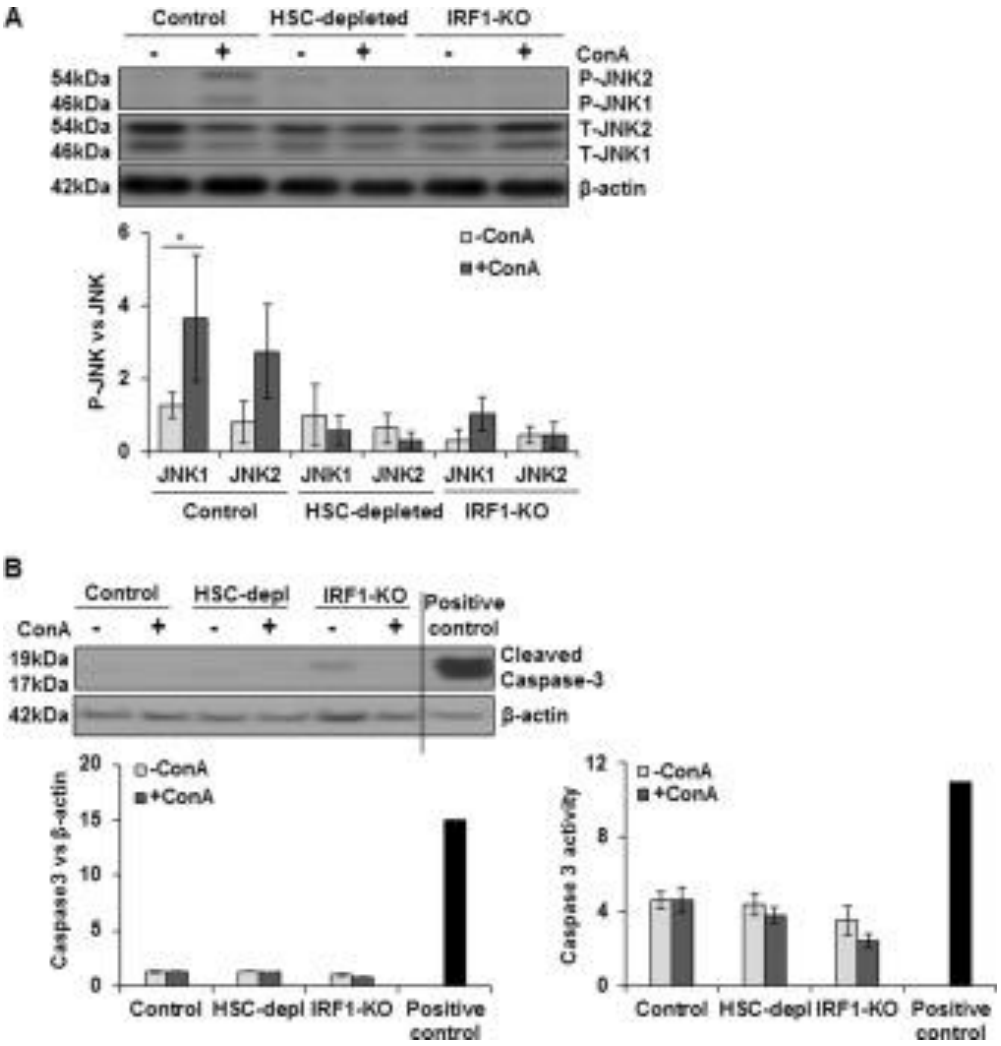

Supplemental Figure S9. Proteins were extracted from livers of vehicle or ConA-treated WT, HSC-depleted or IRF1-KO mice and subjected to Western blot analysis to detect JNK (**A**) and caspase-3 (**B**) activation. WT mice show activation of JNK at 6 hours after ConA administration, which is not evident in HSC-depleted or IRF1-KO mice. ConA-induced caspase-3 activation is not detected in WT, HSC-depleted, or IRF1-KO mice, as determined by Western blot analysis and caspase-3 activity assay. For positive control, liver tissue of mice fed an alcohol-containing Lieber-DeCarli liquid diet was used.[22,23] Data are expressed as means ± SD. $^{*}P < 0.05$. P-JNK, phosphorylated JNK; T-JNK, total JNK.